ELSEVIER

International Journal of Coal Geology 51 (2002) 129–141

International Journal of COAL GEOLOGY

www.elsevier.com/locate/ijcoalgeo

Laser-induced fluorescence microscopy—application to possible high rank and carbonate source rocks

Xianming Xiao [a,*], R.W.T. Wilkins [b], Dehan Liu [a], Zufa Liu [a], Jiaqui Shen [a]

[a] *State Key Laboratory of Organic Geochemistry, Guangzhou Institute of Geochemistry, Chinese Academy of Sciences, Guangzhou 510640, China*

[b] *CSIRO Petroleum, P.O. Box 136, North Ryde, NSW, Australia*

Received 2 July 2001; accepted 5 April 2002

Abstract

It is difficult to obtain useful fluorescence information from coals and source rocks of high maturity by means of conventional fluorescence microscopy due to the low fluorescence intensity of the macerals. A laser-induced fluorescence microscopy (LIFM) designed by the authors was applied to target the problem. An investigation was made by means of this technique on a suite of coals having a range of mean random vitrinite reflectance (VRo) = 0.3–2.5%, and some high maturity source rocks of early Palaeozoic age. The results show that LIFM greatly improves several functions of conventional fluorescent microscopy. LIFM is very sensitive to organic matter in sediments and for the suite of Chinese coals and possible source rocks investigated, considerably extends the maturity range over which visible fluorescence can be observed. The range is extended from about 1.40% to 2.0% VRo for vitrinite of normal composition, from 1.30% to about 1.50% VRo for alginite and other liptinites, and from about 2.5% to 3.2% VRo for organic inclusions and asphalt-absorbed minerals. With LIFM, it was found that the organic matter in some early Palaeozoic carbonates and argillaceous limestones is distributed very unevenly. In these rocks, which are believed to have been significant source rocks, some microregions are very rich in organic matter or contain a large number of organic inclusions although the total organic carbon (TOC) of the whole rock is low. A microchannel network for petroleum expulsion and migration, comprised of grain boundaries, bedding planes and suture textures containing hydrocarbons was revealed in carbonate strata. LIFM of organic matter in rocks should extend the application of organic petrology in petroleum exploration.

Keywords: Laser-induced fluorescence microscopy (LIFM); High rank coals; High maturity source rocks; Carbonate source rocks; Petroleum migration

1. Introduction

Thirty years have passed since the early applications of fluorescence microscopy in coal petrology, and in the organic petrology of source rocks. During this period, there has been continuous effort to improve the technique in order to optimize its performance for different purposes. The current work has focused on the improvement of the light source for fluorescence excitation from organic matter. Since the introduction of the high-pressure mercury lamp in the 1970s, the quantitative measurement of fluorescence

* Corresponding author. Tel.: +86-20-85290176; fax: +86-20-85290706.

E-mail address: xmxiao@gig.ac.cn (X. Xiao).

0166-5162/02/$ - see front matter
PII: S0166-5162(02)00085-X

intensity of liptinite, and sometimes vitrinite in coals and source rocks, has become possible. However, its use is usually confined to vitrinite reflectance (VRo) < 1.30–1.40% for macerals (Teichmüller and Ottenjann, 1977; Stach et al., 1982; Ottenjann et al., 1982) and to VRo < 2.0% for mineral bituminous groundmass and some faunal relics in source rocks (Van Gijzel, 1981). From the late 1980s, the possibility of laser-induced fluorescence excitation was noted and some related techniques have been developed and applied in organic petrology and organic geochemistry. These are pulsed laser fluorescence microscopy for the determination of fluorescence lifetimes (Landis et al., 1987), confocal laser scanning microscopy (Body, 1988; Scott, 1989; Liu and Xiao, 1991; Stasiuk et al., 1998; Stasiuk, 1999a,b), laser fluorescence microprobe (Wilkins, 1995), laser-induced fluorescence of extracts, and in situ laser micropyrolysis-GC-MS (Stout and Lin, 1992; Jin and Qin, 1993; Stout, 1993). However, the conventional high-pressure mercury lamp does not appear to have been replaced by a laser light source to excite fluorescence for direct microscopic observation and fluorescence intensity measurement, and there appear to be no published photographs of macerals taken by this method, although there are examples of fluorescence images of macerals obtained by confocal laser scanning microscopy (Stasiuk, 1999a,b). With the latter technique, however, the fluorescence image is a reconstructed false color image whereas the fluorescence image observed by LIFM is directly observed.

In the investigation of petroleum systems in the large Tarim, Ordos and Sichuan Basins of China, it has been necessary to develop techniques to determine the maturity and source history of early Palaeozoic sediments. Due to the low fluorescence intensity of macerals in source rocks of high maturity using conventional fluorescence microscopy, limited information is usually available on source organic matter distribution, and evidences of hydrocarbon expulsion and migration. In the course of experiments in which the high-pressure mercury lamp was replaced by an argon ion laser on a MP3 photometric microscope, we observed a marked increase in the fluorescence intensity of the organic matter in rocks of medium to high maturity, enabling features to be observed which were not apparent with the conventional apparatus. In the present study, we describe apparatus designed and assembled by the authors, for laser-induced fluorescence microscopy (LIFM; Xiao et al., 2000a), that was used to investigate the fluorescence characteristics of coals of different rank, and high maturity shales and carbonates of early Palaeozoic age. The primary aims of this paper are to present the advantages of the LIFM system over conventional fluorescence microscopy, and to demonstrate its potential for applications in coal petrology and petroleum exploration.

2. Instrumentation and experimental methods

Fig. 1 is a sketch diagram of the LIFM instrumentation. A Leica MP3 microphotometer equipped with

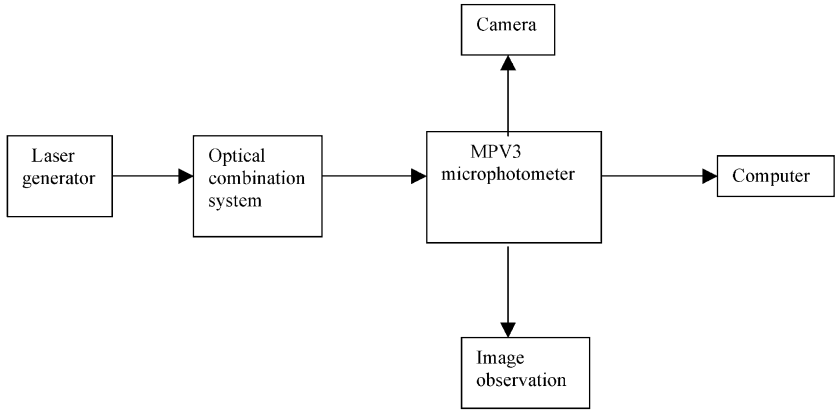

Fig. 1. Sketch diagram showing the combination of components for laser-induced fluorescence microscopy.

an EMI 24561 photomultiplier forms the nucleus of the LIFM system. The light source is a Spectra-Physics Spinnaker 1361 air-cooled argon ion laser chiefly emitting 488 and 514 nm radiation with an all lines maximum power output of 500 mW. The laser beam, introduced into the microscope through the central of three available ports, passes through the correcting lens for the usual diverging light sources causing a slight increase in the divergence of the laser beam. This results in a larger area of the sample surface being irradiated, depending on the objective, compared to the situation in which the essentially parallel beam from the laser passes directly through to the objective. The 488 nm laser line is selected with a standard BP450–490 nm excitation filter and the fluorescence radiation is transmitted through a long pass 510 nm dichroic mirror, with both 500 and 510 nm barrier filters used together for visual observation. A measurement filter was not used. The laser power at the exit of the laser was chosen in the range 100–200 mW according to the sample.

Leitz Fluoresenz water immersion objectives 50/1.0, 25/0.6 and 40/0.75 were selected for use after tests in which oil, water and air media were compared. It was found that immersion oil can dissolve fluorescing substances from sample surfaces causing a rapid dimming of the image. A stronger fluorescence intensity as well as a better image can be obtained with water compared to air medium. The water purified by reverse osmosis membrane used had total dissolved solids less than 1 ppm and no attempt was made to keep it free of oxygen. A pure asphaltene with a brown fluorescence and a weak positive alteration derived from a suberinite-rich lignite (Wilkins et al., 2000) was used as the fluorescence standard, and its initial intensity was set at 100 for the system. For the alteration measurements, an aperture diaphragm was used to define an area with a diameter of 3.5 um, and the fluorescence intensity was measured in unequal intervals with a total excitation period of 600–1200 s. Software for the fluorescence intensity and alteration measurements was modified after the original software of the MPV3 microphotometer. All measurements and operations could be controlled either manually, or through a Legend 586 computer on a Win 97 working platform.

A defect of the optical system is the uneven illumination of the sample surface, due to an interference pattern (laser speckle) originating in the microscope optics. The effect is most prominent on vitrinite and the mottled appearance of the well-polished surface seen in Fig. 2b is an artifact of the pattern. The effect can be greatly reduced by use of a ground glass screen; however, about half the light incident on the sample is lost. For this reason, we recommend that the ground glass screen is not used while scanning the sample for macerals, though when used for photography, the ground glass screen greatly improves the image obtained

3. Samples and maturity

Two sets of samples were involved in this study: coals and possible source rocks. The coals were sampled mainly from the Shanxi Formation of early Permian age in north China, and they cover a wide range of rank with measured VRo of 0.30–2.50%. The possible source rocks were mostly early Palaeozoic, including black and gray shales, argillaceous limestones and carbonates from the Tarim, Ordos, Sichuan and other basins. The TOC values range 0.14–3.65%, Rock-Eval hydrogen index (HI) up to 112 but mostly less than 20 mg/g TOC, and equivalent VRo is within the range 1.10–3.60% (Table 1). All samples were from core. To avoid contamination, the samples were cut into approximately $20 \times 20 \times 30$ mm blocks without mounting in epoxy resin, and polished without the use of oil or solvents.

Equivalent VRo values for the early Palaeozoic samples were determined from the measured reflectances of bitumen and vitrinite-like macerals. Two equations proposed for the relationship between solid bitumen reflectance (BRo) and vitrinite reflectance are:

1. $VRo = 0.668\ BRo + 0.346$ (Liu and Shi, 1994), and
2. $VRo\% = 0.668\ BRo + 0.40$ (Jacob, 1985).

There are small differences of 0.05–0.12% between values of VRo calculated from the two equations through the maturity range of the studied samples. In this paper, we use Jacob's equation for equivalent VRo calculated from measured BRo (Table 1). Equivalent VRo values were also determined from the measured

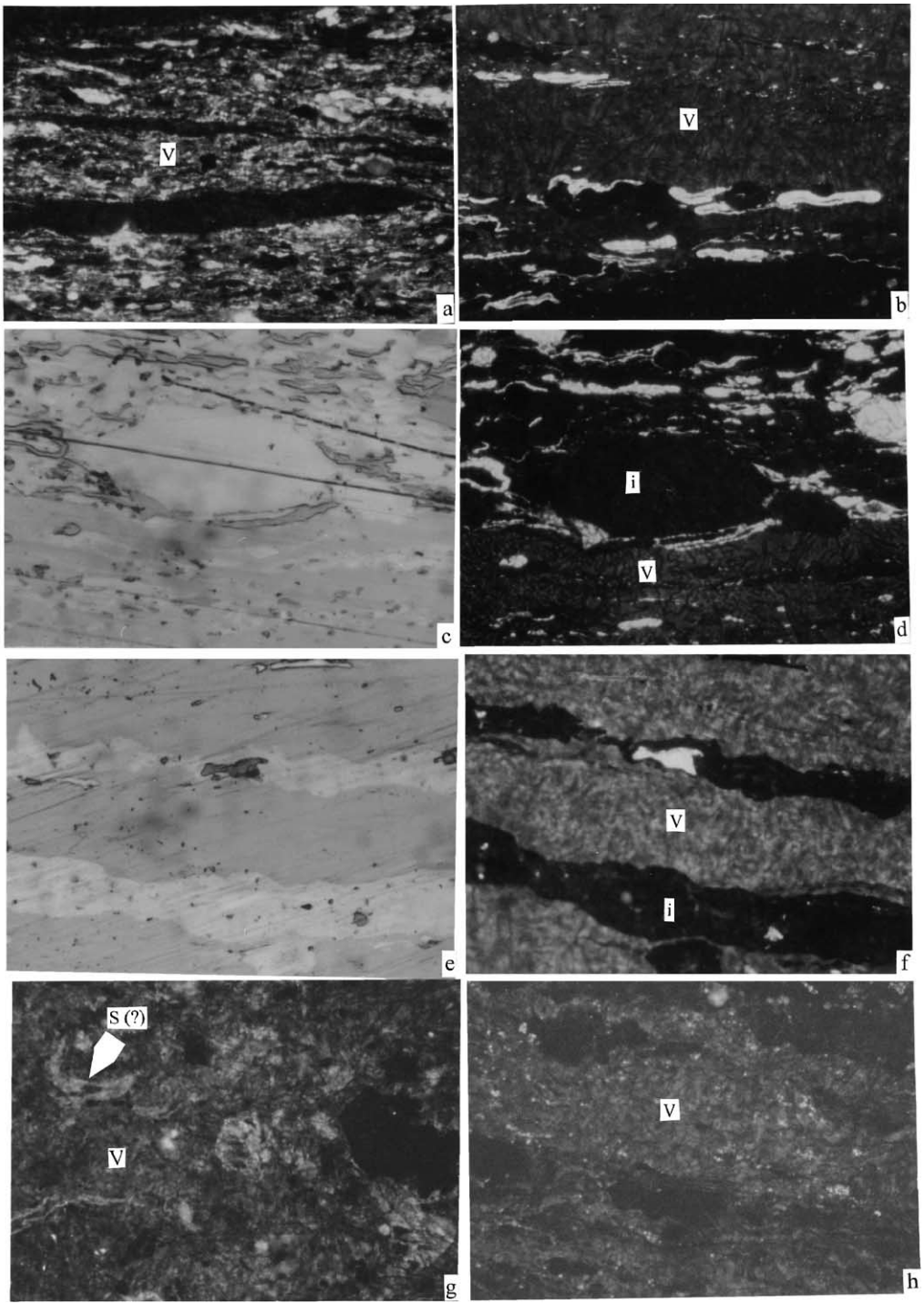
V
a
V
b
c
i
V
d
e
V
i
f
S (?)
V
g
V
h

Table 1
Geological and geochemical data on some typical samples of early Palaeozoic age from Chinese basins

Sample No.	Basin	Well	Depth (m)	Age	Lithology	Equivalent VRo (%)[a]	TOC (%)	S_1 (mg/g TOC)	S_2 (mg/g TOC)	T_{max} (°C)	HI (mg/g TOC)
T-1	Tarim	TZ12	4970	O_{2-3}	Argillaceous limestone	1.10	1.50	0.39	1.68	448	112
T-2	Tarim	TZ12	5075	O_{2-3}	Argillaceous limestone	1.21	1.18	0.21	0.80	446	68
T-3	Tarim	TZ10	4920	O_{2-3}	Argillaceous limestone	1.30	1.05	0.08	0.43	443	41
O-1	Ordos	Er5	2961	O_{1m}	Limestone with microband of shale	1.51	0.30	0.06	0.04	–[b]	13
O-2	Ordos	Yi25	4435	O_{1m}	Lime-dolomite	1.61	0.14	0.24	0.11	449	79
O-3	Ordos	Yi25	4516	O_{1m}	Dolomite	1.68	0.35	0.08	0.02	–	6
T-4	Tarim	Keping	Outcrop	O_2	Shale	1.36	3.65	2.65	4.56	448	110
T-5	Tarim	Keping	Outcrop	O_2	Limestone	1.36	1.09	0.39	1.08	450	99
T-6	Tarim	KN1	4995	ϵ	Silicic limestone	1.76	1.87	0.63	0.19	–	10
T-7	Tarim	KN1	5189	ϵ	Silicic limestone	1.94	1.41	0.17	0.01	–	1
T-8	Tarim	TD-1	4154	O_{2-3}	Mudstone	2.48	1.04	0.0	0.10	–	11
T-9	Tarim	TD-1	4360	O_1	Mudstone	2.53	2.31	0.0	0.23	513	10
T-10	Tarim	TZ1	6505	ϵ	Dolomite	2.4	0.40	0.17	0.08	–	20
T-11	Tarim	TD-1	4811	ϵ	Limestone	3.40	0.86	0.01	0.0	–	0
S-1	Sichuan	GK1	4986	ϵ	Dark gray siltmudstone	2.94	1.43	0.09	0.07	–	5
S-2	Sichuan	GK1	4988	ϵ	Gray carbonate	3.02	0.25	0.02	0.02	–	8
S-3	Sichuan	GK1	5358	Z	Black carbonate	3.00	0.57	0.05	0.01	–	2
S-4	Sichuan	GK1	5356	Z	Mudstone	3.28	1.55	0.05	0.19	–	12
Q-1	Quizhou	Nayong	Outcrop	P_1	Bituminous limestone	3.2	1.86	0.43	0.22	–	12

[a] Equivalent VRo based on bitumen reflectance and vitrinite-like maceral reflectance (see text).
[b] S_2 too low to determine T_{max}.

reflectances in oil medium of vitrinite-like macerals (VLMRo) using the relationships (Xiao et al., 2000c):

$$\mathrm{VRo}\% = 1.26\ \mathrm{VLMRo} + 0.21\ (\mathrm{VLMRo} < 0.75\%);$$

$$\mathrm{VRo}\% = 0.28\ \mathrm{VLMRo} + 1.03\ (\mathrm{VLMRo} = 0.75 - 1.50\%);\ \text{and}$$

$$\mathrm{VRo}\% = 0.81\ \mathrm{VLMRo} + 0.18\ (\mathrm{VLMRo} > 1.50\%).$$

The results for typical samples are presented in Table 1.

4. Results and discussion

4.1. Fluorescence of vitrinite and liptinite in coals

The dark brown fluorescence of vitrinite in some coals has been reported by many authors using conventional fluorescence microscopy (e.g. Ottenjann, 1988; Davis et al., 1990). From previously published data, it seems that in most cases only the desmocollinite submaceral of vitrinite has significant visible fluorescence, and this is usually confined to VRo < 1.30–1.40%. The major advantage of LIFM in microscopy is the much higher intensity of fluorescence emission that can be achieved allowing the fluorescence of all submacerals of vitrinite to be visible over a wider

Fig. 2. Fluorescence of vitrinite and associated liptinite in humic coals of different rank. Polished surface. Note that the uneven fluorescence intensity in the vitrinite images is an artifact due to laser speckle. (a) Vitrinite (v) with yellow-brown fluorescence; Tertiary, Baise Basin, VRo = 0.40%, water immersion, LIFM, × 320. (b) Vitrinite (v) with brown fluorescence, liptinite with yellow fluorescence, and inertinite (i) without fluorescence; Permian, Furan Basin, VRo = 0.76%, water immersion, LIFM, × 320. (c) Coal macerals, reflected light, × 320, Permian, Datong Basin, VRo = 0.60%. (d) The same field as (c), vitrinite (v) with dark brown fluorescence and inertinite (i) without fluorescence, water immersion, LIFM, × 320. (e) Coal macerals, reflected light, × 320, Permian, Pidishan coal mine, VRo = 1.10%. (f) The same field with (e), vitrinite (v) with brown yellow fluorescence and inertinite (i) without fluorescence, water immersion, LIFM, × 320. (g) Vitrinite (v) and sporinite (S?) with brown fluorescence, Taiyun coal mine, Permian, VRo = 1.48%, water immersion, LIFM, × 320. (h) Vitrinite with very weak brown fluorescence, Permian, Puyong Basin, VRo = 2.0%, water immersion, LIFM, × 320.

maturity range. With LIFM, the fluorescence color of vitrinite varies from brown to yellow-brown (Fig. 2a–h) over the maturity range of brown coal to low volatile bituminous coal. Fig. 2h shows that vitrinite in a coal with VRo as high as 2.0% (semianthracite) still has a dark brown fluorescence. However, with further increase in rank, the fluorescence of vitrinite rapidly becomes invisible under the conditions used in the present study.

The stronger fluorescence intensity of vitrinite with LIFM is attributed to the power of radiation on the sample. With the 25/0.6 objective, measured light power at the sample can be more than five times greater with the laser source than with the high-pressure mercury lamp depending on the laser power chosen. We should note that visible fluorescence has also been used as an indicator of perhydrous vitrinite composition (Stach et al., 1982, p. 36). Thus, the range of visible fluorescence of vitrinite is dependent upon its composition as well as the apparatus and operating conditions, and this should be borne in mind when comparing ranges of visible fluorescence in macerals.

Fig. 3 shows the relationship between VRo and the fluorescence intensity of telocollinite from the suite of coals. The overall decrease of I_{600} (fluorescence intensity after 600 s excitation) with increasing VRo is interrupted by a weak broad band centred on VRo = 1.0%. The curve of VRo against I_0 (initial fluorescence intensity) with a minimum at 0.50% and a maximum at about 1.00% is similar to that for

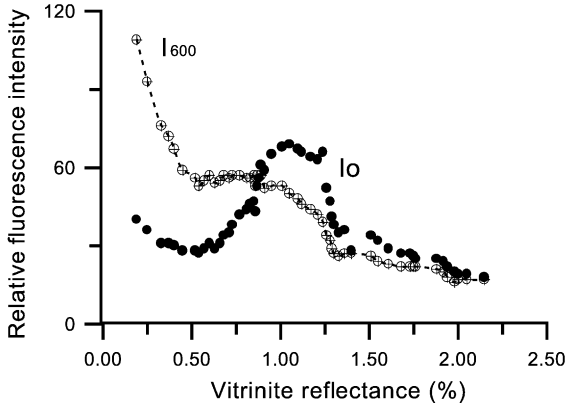

Fig. 3. The relationship of vitrinite reflectance to initial fluorescence intensity (I_0) and fluorescence intensity at 600 s (I_{600}) for Chinese humic coals measured by LIFM.

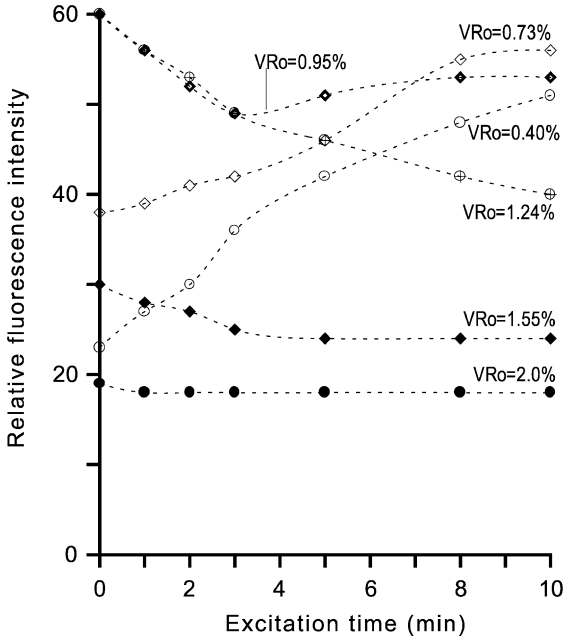

Fig. 4. Fluorescence alteration of vitrinite in coals illustrating the maturity dependence and three types of alteration pattern (see text).

German coals as determined by Ottenjann et al. (1982) using conventional fluorescence microscopy and an air medium. However, the fluorescence intensity of vitrinite at low rank (VRo < 0.5%), is 1–2 orders of magnitude lower in the Chinese coals. Ottenjann et al. (1982) attributed the fluorescence of vitrinite in coals with maturity VRo < 0.50% and >0.50% to primary and secondary fluorescence, respectively. The LIFM data could be interpreted as indicating that the measured fluorescence intensity in the range VRo>0.50% is the sum of decreasing primary and increasing secondary fluorescence. It is important to bear in mind, however, that for both Chinese and German coals, there is a break in the age of the coals near the minimum. In both cases, the coals with VRo < 0.5% are mainly Tertiary whereas those with VRo>0.5% are Palaeozoic. No fluorescence study of a complete rank sequence of coals of either Tertiary or Palaeozoic age is available.

The fluorescence alteration of the telocollinite as observed by LIFM (Fig. 4) is similar to that obtained by laser fluorescence microprobe (Wilkins, 1995) although the laser flux density is different in the two methods and water was used instead of air as a

medium in the present experiments. In both, the alteration ratio R (I_{600}/I_0) passes from positive ($R>1$) to negative ($R<1$) at about VRo = 0.90% (Fig. 3), and R decreases almost linearly between VRo = 0.2% and 1.1% at which point it begins a slight linear increase. The major difference between LIFM and laser fluorescence microprobe results is the smaller fluorescence alteration ratios obtained for low rank samples with LIFM. As both positive and negative alterations are known to originate in photochemical oxidation reactions (Davis et al., 1990; Pradier et al., 1992), presumably there is sufficient partial pressure of oxygen in the water to allow these reactions to take place. The LIFM result is also similar to that obtained by Davis et al. (1990) using conventional fluorescence microscopy and water medium. However, the dual alteration pattern occurs at higher maturity and the negative alteration at the beginning of excitation is stronger for LIFM.

With LIFM, the intense visible fluorescence of much liptinite is not perceptibly different from that seen by conventional fluorescence microscopy (Fig. 2a,b,d). However, the visible fluorescence of some liptinite can be observed in low volatile bituminous coals. For the Chinese coals, the highest rank at which some liptinite (a sporinite-like maceral) with visible fluorescence was found is 1.48% VRo (Fig. 2g). These results show that with LIFM the range of visible fluorescence of both vitrinite and liptinite can be significantly increased compared to conventional fluorescence microscopy.

4.2. Identification of organic matter in source rocks of high maturity

Some Chinese early Palaeozoic sedimentary rocks characterized by high maturity and low content of organic matter, usually with equivalent VRo over 1.10% and a TOC content of 0.20–2.50%, may have been petroleum source rocks. We have found it difficult to use conventional fluorescence microscopy to identify and to determine the distribution of important oil source macerals such as alginite and other liptinites, as well as to investigate mineral bituminous groundmass in relation to petroleum generation and migration in these rocks. Some examples will illustrate how LIFM can assist in overcoming some of these problems.

The early Ordovician carbonates from the north-middle Ordos Basin are at a high stage of maturity. Yellow fluorescing macerals including possible alginite and algae-detrinite were observed in source rocks from this area with an equivalent VRo of 1.51%, by means of the LIFM technique (Fig. 5a). Macerals with a similar level of fluorescence were observed in L.-M. Ordovician black mudstone and argillacous limestone with equivalent VRo of 1.36% from the Keping outcrop of the Tarim Basin (Fig. 5b). In source rocks of higher maturity, such as samples from wells KN-1 and TD-1 of the Tarim Basin with equivalent VRo of 1.70–1.90% and 2.50%, respectively, even with LIFM observation there are no fluorescing macerals (Fig. 5c–e). However, liquid hydrocarbon inclusions and carbonates or other minerals with absorbed asphalt having various fluorescence colors and intensities can be observed (Table 2; Fig. 5c,d,e). The mineral-bituminous groundmass from the samples of both areas has a distinct visible fluorescence (Fig. 5c,d). Some residual organic inclusions with a yellow-brown fluorescence were found in carbonate with equivalent VRo as high as 3.02% from well GK-1 of the Sichuan Basin (Fig. 5f). However, little fluorescence information related to organic matter was obtained from source rocks with higher maturity such as samples of early Permian limestones with an equivalent VRo over 3.20% from the Nayong Basin, and carbonates from well TD-1 of the Tarim Basin.

With the LIFM technique, the mineral bituminous groundmass of source rocks exhibits fluorescence alteration which is maturity-dependent. Three alteration patterns were recorded from the studied samples: negative–positive (dual) alteration, occurring in the range of VRo < 1.60%; negative alteration, in the range 1.60–2.50% VRo; and negative in the first 5 min with no further alteration, in the range VRo>2.50% (Fig. 6). Compared to the alteration patterns observed by Teichmüller and Ottenjann (1977), negative alteration of the mineral bituminous groundmass begins at higher levels of maturity with LIFM. This implies that the LIFM technique is sensitive to very small concentrations of soluble organic matter in rocks.

The above results show that LIFM can extend the maturity range of visible fluorescence for alginite and other liptinites from 1.30% to about 1.50% VRo, and from 2.5% to about 3.20% VRo for organic inclusions and mineral bituminous groundmass.

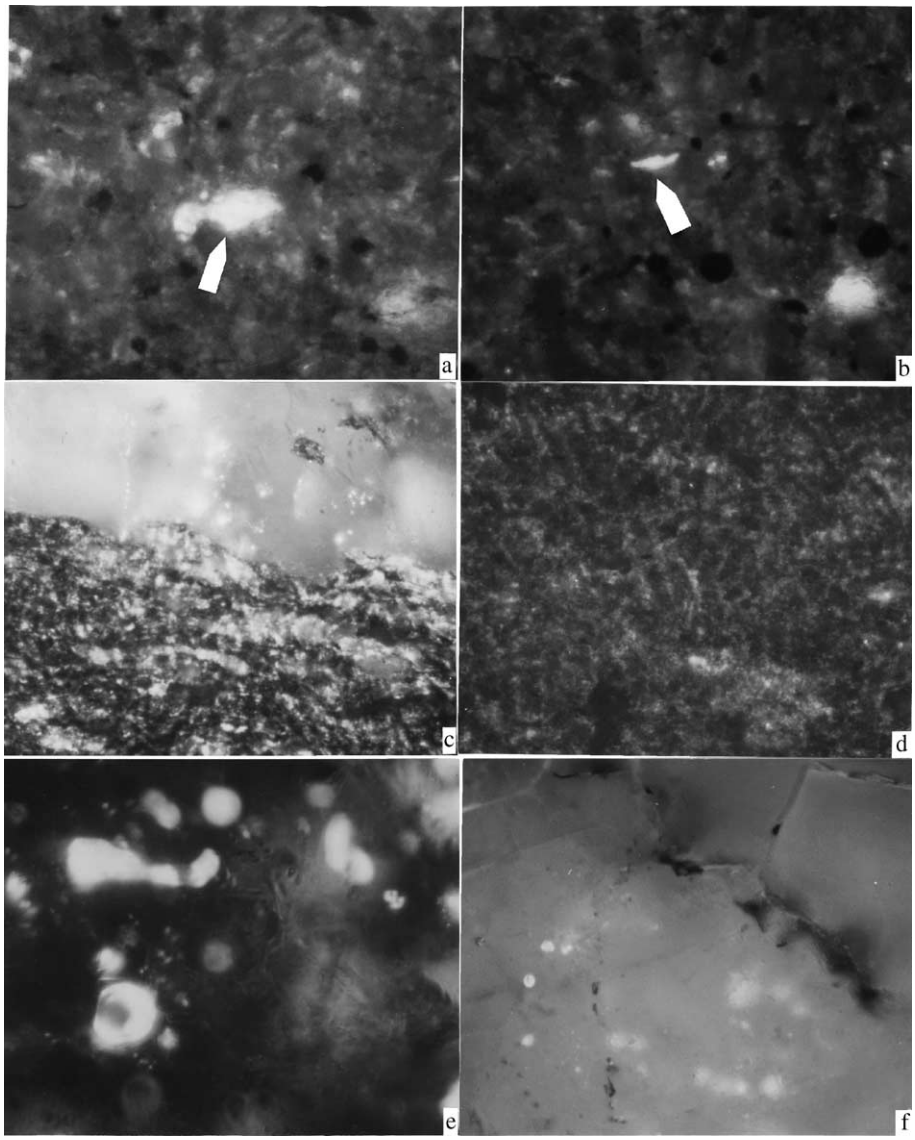

Fig. 5. Fluorescence of macerals and mineral-bituminous groundmass in high maturity source rocks of early Palaeozoic age. Polished surface, water immersion, LIFM, × 320. (a) Macerals (alginite and algae-detrinite) with yellow fluorescence. Sample O-1, limestone with a microband of shale, Ordos Basin, equivalent VRo = 1.51%. (b) Maceral (alginite) with yellow fluorescence in a mineral-bituminous groundmass with yellow-brown fluorescence. Sample T-4, black shale, Keping outcrop, Tarim Basin, equivalent VRo = 1.36%. (c) Mineral-bituminous groundmass with yellow-brown fluorescence (lower part), and organic inclusions with yellow green fluorescence in a micro-lens of carbonate (upper part). Sample T-4, black shale, Keping outcrop, Tarim Basin, equivalent VRo = 1.36%. (d) Mineral-bituminous groundmass with weak yellow-brown fluorescence and no obvious fluorescence alteration. The uneven green fluorescence is caused possibly by prolonged exposure of sample surface to laser to extract soluble organic components, which usually occurs in weak fluorescence samples by the FILM. Sample T-8, dark gray mudstone, Tarim Basin, equivalent VRo = 2.48%. (e) Organic inclusions with yellow-green fluorescence in a calcite vein. Sample T-7, silicic limestone, Cambrian, KN-1, Tarim Basin, equivalent VRo = 1.90%. (f) Residual organic inclusions with brown fluorescence along grain boundaries. Sample S-2, gray carbonate, Sichuan Basin, equivalent VRo = 3.02%.

Table 2
Location and fluorescence of the studied samples

Sample No.	Basin	Well	VRo (%)	Fluorescing macerals	Fluorescence of mineral-bituminous groundmass	Fluorescence of organic inclusion	Fluorescence of asphalt-absorbed mineral
T-1	Tarim	TZ12	1.10	Lamalginite, algae-detrinite	Yellow-green color	Pure liquid hydrocarbon inclusions with yellow-green color	Strong yellow-green or yellow color
T-2	Tarim	TZ12	1.21	Lamalginite, algae-detrinite	Yellow-green color	Pure liquid hydrocarbon inclusions with yellow-green color	Strong yellow-green or yellow color
T-3	Tarim	TZ10	1.30	Lamalginite, algae-detrinite	Yellow-green color	Pure liquid hydrocarbon inclusions with yellow-green color	Strong yellow-green or yellow color
T-4	Tarim	Keping	1.36	Lamalginite, algae-detrinite	Yellow color	Pure liquid hydrocarbon inclusions with yellow-green color	Strong yellow-green or yellow color
T-5	Tarim	Keping	1.36	Lamalginite, algae-detrinite	Yellow-green color	Pure liquid hydrocarbon inclusions with yellow-green color	Strong yellow-green or yellow color
O-1	Ordos	Er5	1.51	Lamalginite, algae-detrinite	Yellow-green color	Organic inclusions with yellow-green fluorescence	Strong yellow-green or yellow color
O-2	Ordos	Yi25	1.61	nf	Yellow-green color	Organic inclusions with yellow-green fluorescence	Strong yellow-green or yellow color
O-3	Ordos	Yi25	1.68	nf[a]	–[b]	Organic inclusions with yellow-green fluorescence	Strong yellow-green or yellow color
T-6	Tarim	KN1	1.76	nf	–	Organic inclusions with yellow-green fluorescence	Strong yellow-green or yellow color
T-7	Tarim	KN1	1.94	nf	–	Organic inclusions with yellow fluorescence	Yellow color
T-8	Tarim	TD1	2.48	nf	Yellow brown color	Organic inclusions with yellow fluorescence	Weak green color
T-9	Tarim	TD1	2.53	nf	Yellow-green color	Organic inclusions with yellow fluorescence	Weak green color
T-10	Tarim	TZ1	2.4	nf	–	Organic inclusions with yellow fluorescence	Weak green color
T-11	Tarim	TD1	3.4	nf	Weak green color	nf	nf
S-1	Sichuan	GK1	2.94	nf	Weak green color	Organic inclusions with weak brown fluorescence	Yellow color
S-2	Sichuan	GK1	3.02	nf	–	Organic inclusions with weak brown fluorescence	Yellow color
S-3	Sichuan	GK1	3.0	nf	–	nf	nf
S-4	Sichuan	GK1	3.28	nf	Weak green color	nf	nf
Q-1	Quizhou	Nayong	3.2	nf	–	nf	nf

[a] Not found.
[b] Little mineral-bituminous groundmass.

The early Palaeozoic strata from some large petroliferous basins in China contain a low content of organic matter, normally with TOC in the range of 0.20–0.50%. For a long time, there have been different opinions on the hydrocarbon potential of these rocks. From the geological perspective, there appear to be insufficient alternative sources with the capacity to form the oil and gas pools discovered in the basins related to this study (Xiao et al., 2000b). From the geochemical viewpoint, some significant source rocks may have a TOC content of 0.50% (Hunt, 1979; Tissot and Welte, 1984). However, these high maturity source rocks, normally with an equivalent VRo>1.20%, have undoubtedly lost an indeterminate amount of organic

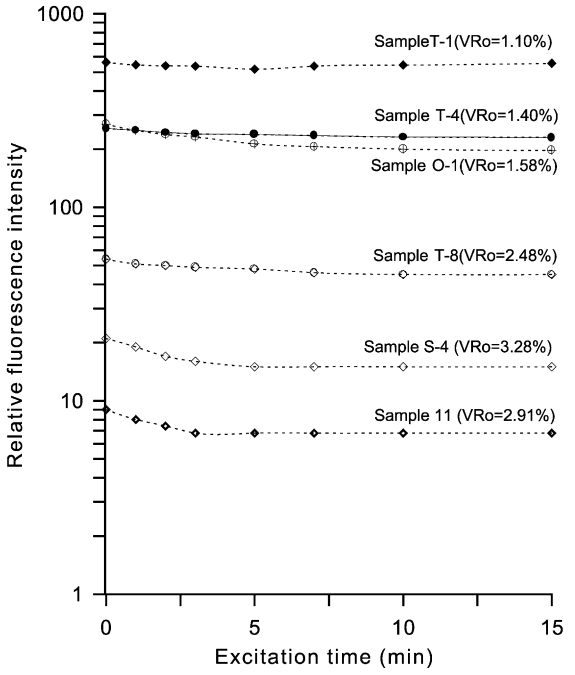

Fig. 6. Fluorescence alteration patterns of mineral bituminous groundmass from source rocks with different maturity. Sample T-1 shows negative–positive (dual) alteration; samples T-4, O-1, and T-8 negative alteration; and samples S-4, T-11 have negative alteration for the first 5-min excitation, followed by almost no change.

carbon during maturation so that their initial TOC values could have been much higher. Thus, it is an important task to investigate the nature and distribution of the remaining source organic matter in these rocks. In comparison with conventional fluorescence microscopy, the higher fluorescence intensity obtained with LIFM observation enables the residual organic matter to be better evaluated and hydrocarbon generation to be investigated through hydrocarbon inclusions.

A set of the samples with TOC of 0.20–0.50% from the Tarim Basin and the Ordos Basin was investigated by LIFM. The results show that source organic matter is very unevenly distributed. Some microregions, very rich in organic matter, contain fluorescing macerals, and fluorescent mineral-bituminous groundmass associated with a large number of organic inclusions can be observed (Fig. 5). Some of the samples with TOC of 0.30–0.50% from well GK-1 in the Sichuan Basin were found to contain significant concentrations of bitumen (Liu and Xiao, 2000), organic inclusions and fluorescing minerals with absorbed asphalt (Fig. 5f). It is believed that these rocks were significant source rocks, generating and expelling petroleum during their geological history, although their present whole rock TOC is usually not high. These results show that it is important for an objective evaluation of high maturity early Palaeozoic source rocks to include not only geochemical data such as TOC, Rock-Eval, PY-GC, but also petrographic information from LIFM and other methods.

4.3. Microscopic observations related to petroleum expulsion and migration in carbonates

Because carbonates have active chemical properties leading to rapid diagenesis, carbonate source rocks behave differently to mudstone source rocks in hydrocarbon expulsion and migration. It has been proposed (Durand, 1983; Ungerer et al., 1987) that water saturation in mudstone source rocks during burial, compaction and diagenetic evolution, including dehydration of the clay minerals, must be sufficiently reduced by expulsion before the flow of a separate hydrocarbon phase becomes possible. However, there is no generally accepted idea for the processes and mechanism of hydrocarbon expulsion and migration in carbonate source rocks, and limited microscopic information appears to be available. Three interesting features of relevance to hydrocarbon expulsion and migration in carbonate source rocks have been commonly observed in our LIFM studies.

(1) A micronetwork system was shown by fluorescing mineral-absorbed asphalt between mineral grains (Fig. 7a,b). The micronetwork width varies from less than 0.20 μm to more than 2.0 μm. It is in fact a microchannel way, sometimes filled with clay minerals, pyrite grains and pyrobitumen along the boundaries of the mineral grains. This indicates that the micronetwork system is a pathway for hydrocarbon expulsion and migration in carbonate source rocks during diagenetic evolution.

(2) Plane surfaces approximately parallel to bedding are well developed in the carbonate samples. Lines or bands of yellow fluorescing asphalt as seen in polished section show that hydrocarbons migrated along plane surfaces such as those that are particularly well developed in lamellar carbonates from the Ordos Basin (Fig. 7c). They connect the micropores in carbonate source rocks.

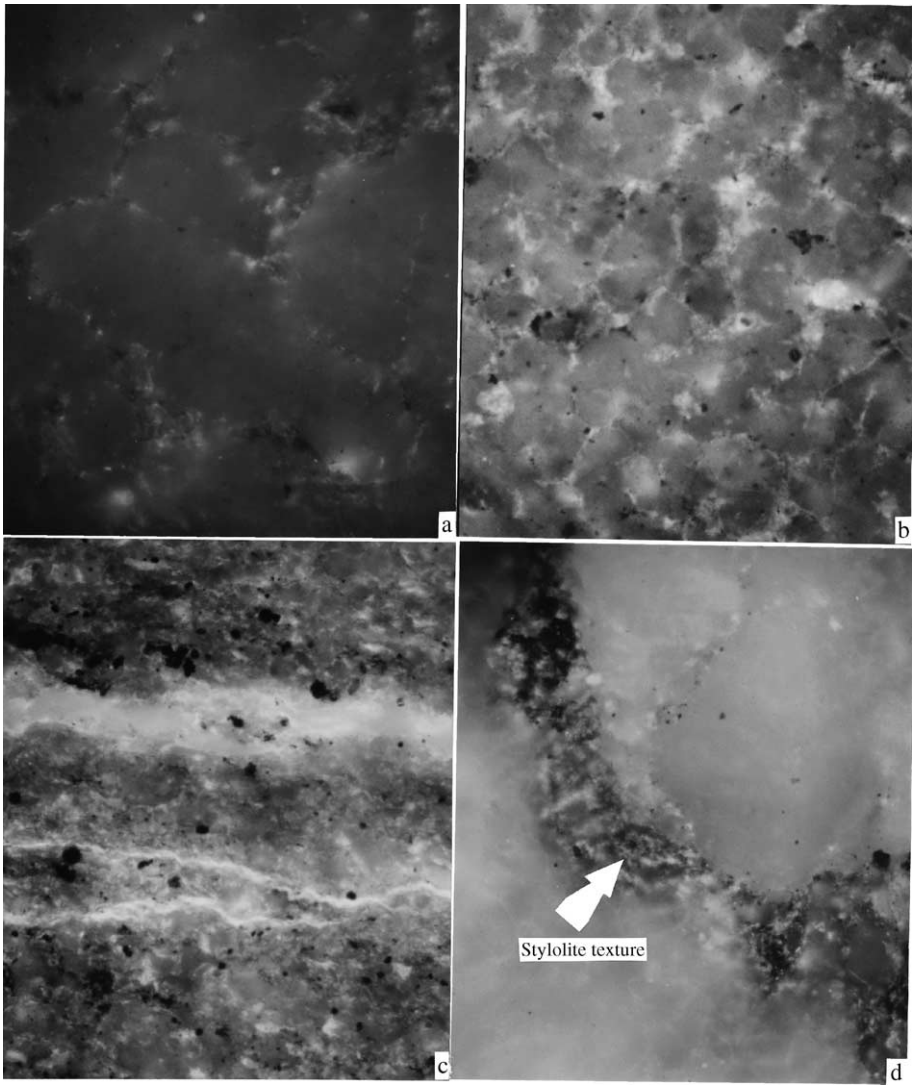

Fig. 7. Microchannel system of hydrocarbon primary migration in carbonates. Polished surface, water immersion, LIFM, × 320. (a) Micropores along carbonate grain boundaries, filled with hydrocarbons showing stronger yellow fluorescence. Sample T-5, dark gray carbonate, Keping outcrop, Tarim Basin, equivalent VRo = 1.36%. (b) Micropores along carbonate grain boundaries, filled with hydrocarbons showing stronger yellow fluorescence. Sample O-1, dark gray limestone, Ordos Basin, equivalent VRo = 1.51%. (c) Planar surfaces near a carbonate/shale boundary filled by migration hydrocarbon, showing a bright yellow fluorescence. Sample O-1, limestone with a microband of shale, Ordos Basin, equivalent VRo = 1.51%. (d) Stylolite texture, filled by hydrocarbon, showing yellow-brown fluorescence. Sample T-3, argillaceous limestone, Lower Ordovician, TZ-12, Tarim Basin, equivalent VRo = 1.30%.

(3) Stylolite textures are commonly formed in carbonates by pressure solution during diagenesis (Renard et al., 1997; Heydari, 2000). Fig. 7d shows stylolites filled by yellow-brown fluorescing hydrocarbon, indicating they form very important channel ways for hydrocarbon migration in carbonates.

5. Conclusions

The use of an argon ion laser as a light source (LIFM) instead of the conventional high-pressure mercury lamp can enhance the value of fluorescence microscopy for the study of organic matter in high

maturity samples. Using this approach, an investigation of some typical Chinese coals and early Palaeozoic source rocks of high maturity has shown:

(1) LIFM is a sensitive means of characterizing organic matter, including both kerogen and soluble organic matter in rocks. Organic matter in even trace amounts is sufficient to produce a visible fluorescence over a wide maturity range.

(2) A significant extension of the maturity range for visible fluorescence was recognized using LIFM. Visible fluorescence is extended to 2.0% VRo for vitrinite, about 1.50% VRo for alginite and liptinite, and to about 3.0% VRo for organic inclusions and minerals with absorbed asphalt.

(3) The patterns of alteration of fluorescence intensity with time for vitrinites, mineral-bituminous groundmass can be conveniently studied by LIFM. Results suggest that with this experimental design fluorescence alteration proceeds in a similar manner and to a similar degree as with conventional fluorescence microscopy.

(4) The fluorescence information obtained from LIFM is very useful in assessing whether early Palaeozoic carbonates and argillaceous limestones with low TOC content from petroleum-bearing basins in China had been source rocks.

Acknowledgements

The authors are indebted to Dr. Stasiuk and an anonymous reviewer for their constructive comments and suggestions on the original manuscript, and to Dr. Hower for editing this paper. This research is part of the project study on Formation of Oil and Gas Pools Related to Coal Measures conducted and supported by the Chinese Academy of Sciences (kzcx2-110). It has also been supported by National Natural Science Foundation of China (NSFC Grant No.40072043).

References

Body, A., 1988. Confocal optical microscopy. Microscopy and Analysis 7, 7–13.

Davis, A., Rathbone, R.F., Lin, R., Quick, J.C., 1990. Observations concerning the nature of maceral fluorescence alteration with time. Organic Geochemistry 16, 897–906.

Durand, B., 1983. Present trends in organic geochemistry in research on migration of hydrocarbons. In: Bjorøy, M., et al. (Eds.), Advances in Organic Geochemistry 1981. Wiley, Chichester, pp. 117–128.

Heydari, E., 2000. Porosity loss, fluid flow, and mass transfer in limestone reservoirs: application to the Upper Jurassic Smackover Formation, Mississippi. American Association of Petroleum Geologists Bulletin 84 (1), 100–118.

Hunt, J.M., 1979. Petroleum Geochemistry and Geology. Freeman, San Francisco, 617 pp.

Jacob, H., 1985. Disperse solid bitumens as an indicator for migration and maturity in prospecting for oil and gas. Erdöl und Kohle 38, 365–366.

Jin, K., Qin, N., 1993. Application of laser-induced fluorescence of coal extracts for determining rank. Organic Geochemistry 20 (6), 687–694.

Landis, C.R., Sullivan, G.W., Pleil, M.W., Borst, W.L., Crelling, J.C., 1987. Pulsed laser fluorescence microscopy of coal macerals and dispersed organic material. Fuel 66, 984–991.

Liu, D.H., Shi, J.C., 1994. Evaluation of early Palaeozoic carbonate source rocks. Natural Gas Industry 14 (6), 32–36 (in Chinese).

Liu, D., Xiao, X., 1991. The applications of confocal laser scanning microscopy in source rock evaluation. Acta Sedimentologica Sinica 9, 147–150 (in Chinese, with English Abstract).

Liu, D., Xiao, X., 2000. Hydrocarbon potential evaluation of early Paleozoic strata from the Sichuan Basin. An internal report of Chinese state key project (95-110-04-01-01). Guangzhou Institute of Geochemistry, Chinese Academy of Sciences, Guangzhou, pp. 23–25 (in Chinese).

Ottenjann, K., 1988. Fluorescence alteration and its value for studies of maturation and bituminization. Organic Geochemistry 12 (4), 309–321.

Ottenjann, K., Wolf, M., Wolf-Fischer, E., 1982. Das Fluoreszenzverhalten der Vitrinite zur Kennzeichnung der Kokungseigenschaften von Steinkohlen. Glückauf-Forschungshefte 43, 173–179.

Pradier, B., Landais, P., Rochdi, A., Davis, A., 1992. Chemical basis of fluorescence alteration of crude oils and kerogens: II. Fluorescence and infrared micro-spectrometric analysis of vitrinite and liptinite. Organic Geochemistry 18, 241–248.

Renard, F., Ortoleva, P., Gratier, J.P., 1997. Pressure solution in sandstones: influence of clays and dependence on temperature and stress. Tectonophysics 280, 257–266.

Scott, A.C., 1989. Geological application of laser scanning microscopy. Microscopy and Analysis 3.

Stach, E., Mackowsky, M-Th., Teichmüller, M., Taylor, G.H., Chandra, A.D., Teichmüller, R., 1982. Stach's Textbook of Coal Petrology, 3rd edn. Gebrüder Borntraeger, Berlin.

Stasiuk, L.D., 1999a. Confocal laser scanning fluorescence microscopy of Botryococcus alginite from boghead oil shale, Boltysk, Ukraine: selective preservation of various micro-algal components. Organic Geochemistry 30, 1021–1026.

Stasiuk, L.D., 1999b. Microscopic studies of sedimentary organic matter: key to understanding organic-rich strata, with Paleozoic examples from Western Canada. Geoscience Canada 26, 149–172.

Stasiuk, L.D., Tomica, M., Wong, J., Pratt, K., 1998. Fluorescence

confocal laser scanning microscopy of dispersed organic matter in hydrocarbon source rocks. Poster and Abstract, Fifteenth Annual Meeting of The Society for Organic Petrology, Halifax, Abstracts and Program, p. 88.

Stout, S.A., 1993. Lasers in organic petrology and organic geochemistry: II. In-situ laser micropyrolysis-GC-MS of coal macerals. International Journal of Coal Geology 24, 309–331.

Stout, S.A., Lin, R., 1992. Lasers in organic petrology and organic geochemitry: I. Laser-induced fluorescence, thermal extraction, and pyrolysis. Organic Geochemistry 18 (3), 229–239.

Teichmüller, M., Ottenjann, K., 1977. Liptinite und lipoide Stoffe in einem Erdölmuttergestein. Erdöl und Kohle 30, 387–398.

Tissot, B.P., Welte, D.H., 1984. Petroleum Formation and Occurrence, 2nd edn. Springer-Verlag, Berlin, pp. 487–495.

Ungerer, P., Doligez, B., Chenet, P.Y., Burrus, J., Bessis, F., Lafargue, E., Giroir, G., Heum, O., Eggen, R., 1987. A 2D model of basin scale petroleum migration by two phase fluid flow. Application to some case studies. In: Doligez, B. (Ed.), Migration of Hydrocarbon in Sedimentary Basins. Editions Technip, Paris, pp. 415–456.

Van Gijzel, P., 1981. Applications of the geomicrophotometry of kerogen, solid hydrocarbons and crude oils to petroleum exploration. In: Brooks, J. (Ed.), Organic Maturation Studies and Fossil Fuel Exploration. Academic Press, London, pp. 351–377.

Wilkins, R.W.T., 1995. Should fluorescence alteration replace vitrinite reflectance as a major tool for thermal maturity determination in oil exploration? Organic Geochemistry 22, 191–209.

Wilkins, R.W.T., Xiao, X., Liu, Z., 2000. Asphaltene as a standard for fluorescence alteration studies. TSOP Newsletter 17 (1), 6–10.

Xiao, X., Liu D., Shen, J., 2000a. Method to combine a laser-induced fluorescence microscopy. Chinese Patent, 00114099X.

Xiao, X., Song, Z., Liu, D., Lui, Z., Fu, J., 2000b. The Tazhong hybrid petroleum system, Tarim Basin, China. Marine and Petroleum Geology 17 (1), 1–12.

Xiao, X., Wilkins, R.W.T., Liu, D., Liu, Z., Fu, J., 2000c. Investigation of thermal maturity of lower Palaeozoic hydrocarbon source rocks by means of vitrinite-like maceral reflectance. Organic Geochemistry 31 (10), 1041–1052.